46th Annual Review of Progress
in Quantitative Nondestructive Evaluation
QNDE2019
July 14-19, 2019, Portland, OR, USA

QNDE2019-1234

IN-FLIGHT DETECTION OF BEARING FAULTS IN UNMANNED AERIAL VEHICLES

Portia Banerjee[1], Wendy A. Okolo[2], Andrew J. Moore[3]
[1] SGT Inc., NASA Ames Research Center, Moffett Field, CA.
[2] NASA Ames Research Center, Moffett Field, CA.
[3] NASA Langley Research Center, Hampton, VA.

ABSTRACT

Bearing faults is one of the primary causes of motor failure. Due to the frequency of occurrence and high risk associated with intrinsic components, identification and characterization of bearing faults via nondestructive evaluation (NDE) methods have been studied extensively and vibration analysis has been found to be a promising technique for early detection. However, majority of the existing techniques rely on vibration sensors attached onto or in close proximity to the motor in order to collect signals with a relatively high SNR. Due to weight and space restrictions, these techniques cannot be used in unmanned aerial vehicles (UAV), especially during flight since accelerometers cannot be attached to motors in small UAVs. Inertial measurement units (IMUs) attached to the body frame of a UAV measure vibrations experienced by the entire UAV due to multiple factors such as weather conditions, control system characteristics, or propeller imbalances. Hence bearing fault signatures get buried under noisy signals. This paper presents a detailed discussion of typical challenges faced with in-flight detection of bearing failure in UAVs using existing sensors and offers potential solutions to bridge the gap of research in the current state-of-art.

Keywords: bearing, UAV, accelerometers, gyroscope, FFT.

1. INTRODUCTION

The integration of small unmanned aerial vehicles (UAVs) for delivery of goods and medical supplies, surveillance, weather monitoring, precision agriculture, and many other applications is expected to change the national airspace [1, 2]. A systematic approach is thus required for diagnosis and prognosis of UAV health in order to enable efficient and safe operations of the low-altitude airspace. One of the critical components in UAV systems are the motors that consist of movable parts called bearings which undergo fatigue over time leading to motor failure. Current practice for ensuring safety of the motors includes a prescribed pre-flight and post-flight inspection of the UAV followed by replacement of the bearing parts if a motor is 'felt' to be warmer or noisier than its counterparts [3]. Although bearings, like any component undergoing fatigue, are not supposed to fail instantaneously in a short flight of 1-2 hours, lack of in-flight monitoring and highly subjective nature of the prescribed checks occasionally lead to unprecedented motor failures [4]. Besides, external environmental factors such as moisture or dirt could affect the motion of a bearing during a UAV flight. A failed motor is often detrimental since space and weight restrictions do not allow for redundant motors on a small-sized UAV. As a result, current practice relies on periodic replacement of parts which is not only cost inefficient but risks continued use of damaged motors in a UAV.

Majority of existing research [5-6] validates bearing fault detection methods on experimental vibration data from health monitoring testbeds wherein accelerometers are attached to the motor frame. This paper presents an overview of existing studies on bearing fault detection on such datasets. Further, typical accelerometer signals measured by an IMU from a UAV flight with faulty bearings are depicted and compared with lab data. Features from faulty bearings are extracted based on time-frequency representation and a possible in-flight detection approach is demonstrated.

2. BEARING FAULT DIAGNOSIS IN IMS DATA

In order to study the real defect growth process in industrial machinery, bearing run-to failure tests were performed by the Center for Intelligent Maintenance Systems (IMS) at the University of Cincinnati, under normal load conditions on a specially designed test rig [6]. The test rig consisted of four bearings on one shaft driven by an AC motor. Accelerometers were attached onto each bearing using adhesives, as depicted in Fig. 1.

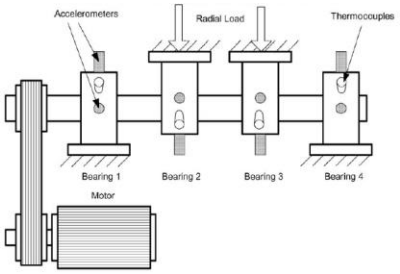

FIGURE 1. Schematic of bearing test rig from IMS [5].

[1] Contact author: portia.banerjee@nasa.gov

The vibration data for all four bearings along with additional details of the test set up is available in the NASA Ames Prognostic Center of Excellence dataset repository [7]. Vibration data was collected every 20 minutes at a sampling rate of 20 kHz by a National Instruments DAQCard-6062E data acquisition device. Damage to the rolling ball in bearing 4 took 35 days to mature from its healthy state to complete failure. Since bearings are rolling components, any damage in the bearing shows up as a periodic pattern in the vibration signal which can be extracted from its frequency spectrum. Vibration signals from the accelerometer attached to bearing 4 are depicted in Fig. 2. The corresponding power spectral density (PSD) at different frequency components indicates clear distinction between the healthy and faulty bearing.

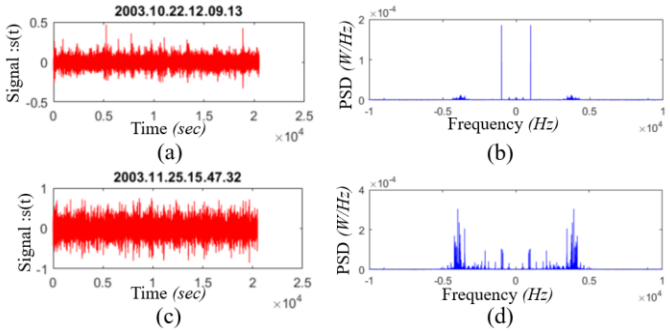

FIGURE 2. Vibration signal from bearing 4 and its power spectral density at different frequency components: (a)-(b) healthy (c)-(d) at failure.

In order to study the damage propagation over the entire 35 days, the PSD of the vibration signal was computed and then the 7 frequencies with highest PSD values were plotted in Fig. 3. It can be observed that the most damage growth signatures are captured by the 5th, 6th and 7th frequencies and not by the highest PSD frequencies since the defect information is suppressed by the natural modal components of the bearing in them.

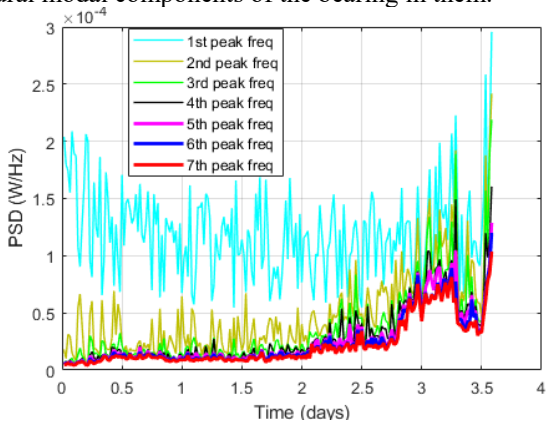

FIGURE 3. Power density at first 7 peak frequency components of bearing 4 vibration data.

Bearings exhibit a weak degradation trend for the majority of their life until there is an abrupt indication of fault towards end-of-life (EOL). As a result, although peak frequencies and associated PSD values may be sufficient features to discriminate bearing health at the beginning and end of its life, classification using these features during shorter time periods within the life cycle becomes challenging. Fig. 4 represents the feature space formed by 5th-10th highest PSD values for 6 to 3 hours before EOL of the faulty bearing. It can be observed that these features overlap during this period. Since we are interested in the bearing health degradation in a UAV flight which typically lasts for a short time period of 1-2 hours, these features of the vibration signal are deemed not suitable for in-flight diagnosis of bearing faults.

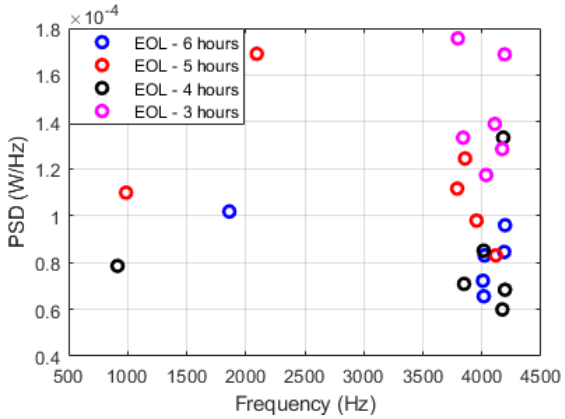

FIGURE 4. Feature space for classifying different states of health of bearing within 3-6 hours of its EOL.

3. BEARING FAULT DIAGNOSIS IN UAV SYSTEM

The goal of our study is to diagnose bearing damage using existing sensors from commercial models of UAVs without having information of the motor's state of health at the beginning of the flight. UAV flight experiments were performed at the NASA Langley Research Center on DJI S-1000 octocopter with faulty bearings on one of the motors. The UAV flights in the experiment were safely stopped before the bearing reached total failure in order to avoid an incident or damage to the UAV. Unexpected noise during the flight indicated degradation of motor health which was later identified as bearing faults from offline inspection. Experimental data from inertial measurement units (IMUs) comprising accelerometer, gyroscope, and magnetometer, installed on the body of the UAV is analyzed in this study for detection of bearing failures.

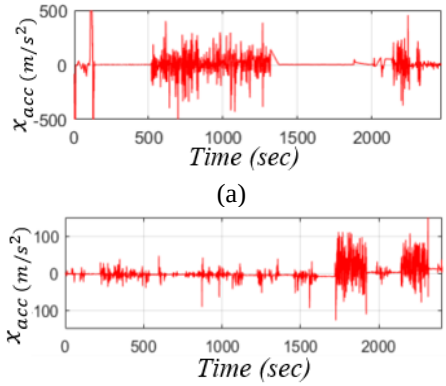

FIGURE 5. Accelerometer data in x-direction from (a) healthy UAV flight (b) UAV with faulty bearing.

Fig. 5 depicts vibration signals along the x-direction as measured by the accelerometer for (a) a healthy UAV and (b) a UAV with faulty bearings.

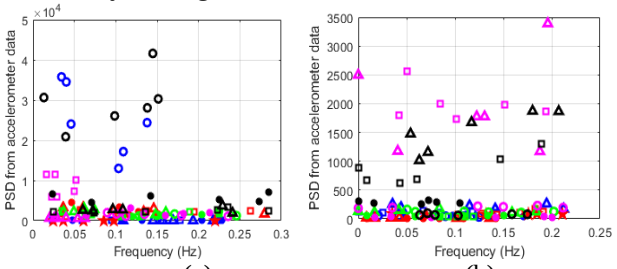

(a) (b)

FIGURE 6. Frequency-power density features at different time windows of (a) healthy and (b) faulty bearing signal. Red: 0-500 sec, Blue: 501-1000 sec, Green: 1001-1500 sec, Black: 1501-2000 sec, Pink:2001-2500 sec.

Features similar to those used in the IMS data analysis were extracted from the accelerometer data. For generating the feature space in Fig. 6, the entire flight of 2500 seconds was divided into 5 sections of 500 seconds each whose features are respectively denoted by red, blue, green, black and pink colors starting from beginning to end of flight. Each section is further segmented into 4 windows of 125 seconds each. The PSD was computed for each windowed signal and the 5^{th}-10^{th} frequencies with highest PSD values were plotted with a set of symbols of a particular color in Fig. 6. A set of four consecutive windows are marked using the same color in the plot representing the 5 sections of the entire time-signal. The red markers indicate features from the initial 500 seconds (~8 min) of the UAV flight whereas the pink markers indicate the last 8 minutes of the UAV flight (bearing fault indications are present during this time window). In the healthy UAV, no discrimination is observed between features from beginning and end of the flight whereas in Fig. 6(b), when the UAV experiences a faulty bearing towards the end of its flight, features denoted by black and pink colors show some separation with features extracted from previous sections of the signal.

In order to improve feature separation and therefore detection capability using on-board sensors, data from the gyroscope is analyzed in addition to the accelerometer power densities. Gyroscopes measure the rotational vibration of the UAV along its x, y, and z axes. The motivation behind using gyroscope data as an additional feature is that if one motor in a UAV fails, the angular motion of the UAV body along its axis will be affected instantaneously before the control system can restabilize and control. Figure 7 represents the PSD signals for the same two UAV flights in an accelerometer-gyroscope feature space, with color assigned according to same time windowing used in Figure 6. It can be concluded that in a healthy state, the PSD-frequency features from both accelerometer and gyroscope form tight clusters whereas once the bearing begins to show indications of failure, the features become an outlier to existing clusters. Detection of outliers in the feature space can be an indication of a potential faulty bearing during the UAV flight.

4. CONCLUSION

This paper presents a comparison of bearing fault diagnosis methods on a public dataset and from flight experiments on commercial UAVs with known faulty bearings. NDE diagnostic methods, which have been validated on public datasets, cannot be directly implemented for in-flight detection of bearing faults in UAVs. In this paper, we utilize gyroscope data as an additional feature and demonstrate the analysis on the UAV flight data. It is important to note that unsupervised learning methods should be employed since the pre-flight motor health may be unknown and no training data may be available.

As a future direction of this research, data from other sensors in the UAVwill be investigated for identifying early indication of a degrading motor bearing. Other time-frequency representations such as matching pursuit decomposition or wavelets can be employed to extract suitable damage-sensitive features.

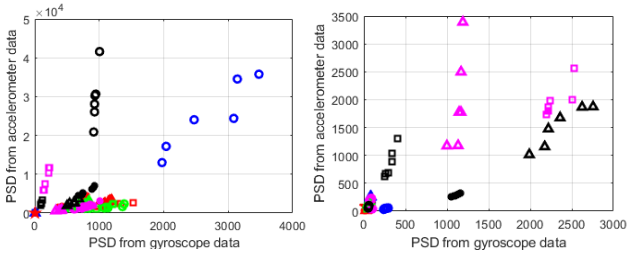

(a) (b)

FIGURE 7. Accelerometer-Gyroscope PSD features at different time windows of (a) healthy and (b) faulty bearing signal.

ACKNOWLEDGEMENTS

This work was supported by the System-Wide Safety (SWS) project under the Airspace Operations and Safety Program within the NASA Aeronautics Research Mission Directorate (ARMD).

REFERENCES

[1] Forecast, FAA Aerospace. "Fiscal Years 2016-2036." Federal Aviation Administration (2016).

[2] Kopardekar, Parimal, et al. "Unmanned aircraft system traffic management (utm) concept of operations." (2016).

[3] Byers, Charles Calvin, and Gonzalo Salgueiro. "Pre-flight self-test for unmanned aerial vehicles (UAVs)." U.S. Patent No. 9,540,121. 10 Jan. 2017.

[4] Freeman, Paul Michael. "Reliability assessment for low-cost unmanned aerial vehicles." (2014).

[5] Wang, Xiang, et al. "Bearing fault diagnosis based on statistical locally linear embedding." Sensors 15.7 (2015): 16225-16247.

[6] Qiu, Hai, et al. "Wavelet filter-based weak signature detection method and its application on rolling element bearing prognostics." Journal of sound and vibration 289.4-5 (2006): 1066-1090.

[7] J. Lee, H. Qiu, G. Yu, J. Lin, and Rexnord Technical Services (2007). IMS, University of Cincinnati. "Bearing Data Set", NASA Ames Prognostics Data Repository